MRI morphometry of the neocortex in patients with periventricular nodular heterotopia

Anton Plavski

Integrated Program in Neuroscience

McGill University, Montreal, Canada

June 2016

A thesis submitted to McGill University in partial fulfillment of the requirements for the degree of Master's of Science

© Anton Plavski, 2016

Acknowledgements

First and foremost, I am grateful beyond what can be expressed with words for the courage and dedication of my relatives – in particular my grandparents and their own parents, grandparents and other relatives – who, with God's help, have endured unfathomable hardships in defending our motherland so that I am alive today to write these words and complete my degree.

Спасибо (пра)деду за победу! Никто не забыт, ничто не забыто!

Many thanks to my thesis supervisor, Dr. Neda Ladbon-Bernasconi, for trusting me and taking me under her supervision. Her guidance and her advice have been instrumental in completing my thesis, and acted as a likeness of Ariadne's thread in directing me along the right path.

I would also like to thank the other members of my advisory committee, Dr. Andrea Bernasconi and Dr. Jeffery Hall, as well as my mentor, Dr. Kenneth Hastings, for likewise taking the time to provide valuable advice at key moments throughout my progression. I thank Dr. Simon Ducharme, my thesis examiner, for his time and advice.

I thank the staff that have kept the Integrated Program in Neuroscience organized and functioning, and the innumerable people who have worked behind the scenes at the Montreal Neurological Institute and at McGill to ensure everything went well.

I thank my laboratory colleagues with whom I have worked for two years for their mentorship (especially Dr. SeokJun Hong), their help, their advice, and simply their enjoyable company. Good and fun times have been had, fond memories will remain.

My friends beyond the laboratory environment have – sometimes without realizing it – kept me motivated for these past two years. Humorous moments have alternated with insightful debates on a vast variety of topics. I owe my personal development during this period in great part to them.

My greatest gratitude goes to my family, particularly to my closest relatives: my mother and my father. They have relentlessly supported me, providing encouragement and emotional abutment whenever such was necessary. They gave me the strength to persevere until the completion of my thesis. Among the other members of my close family, my grandmother and my grandfather especially have offered such support. I do not believe in myself; I believe in my family who believes in me.

Related Publications

Manuscript in preparation.

Abstract

Background. Human corticogenesis is broadly divided into three phases: proliferation, migration and cortical organization. Accordingly, a defect in any of these phases results in a malformation of cortical development (MCD). By allowing the *in vivo* visualization of MCDs, magnetic resonance imaging (MRI) has been instrumental in their classification. One such MCD is gray matter heterotopia (GMH), defined as out-of-place masses of gray matter (GM) – termed "nodules" – containing neurons that have failed to migrate to their intended destination. Such nodules have variable presentation in terms of location, lateralization, size and spread in the brain.

Three distinct subtypes of GMH have been recognized: periventricular nodular heterotopia (PVNH), subcortical heterotopia, and band heterotopia. The focus of my Master's project is specifically the PVNH subtype of GMH. As all types of GMH, PVNH is highly epileptogenic, and the epilepsy is often drug-resistant.

Purpose. To quantify whole-brain changes in cortical thickness and curvature in PVNH, and to assess the spatial relationship between nodules and regions of change.

Methods. We obtained T1-weighted (1 x 1 x 1 mm³) images in 41 patients with PVNH and 41 controls on 1.5T- and 3T-scanners. Patients were further divided into unilateral (UL) *vs*. bilateral (BL) PVNH. Images were registered into stereotaxic space to adjust for differences in brain volume and orientation. We manually mapped the location of nodules,

and algorithmically extracted whole-brain neocortical thickness and curvature. We used whole-brain linear modeling to perform group-wise statistics.

Results. Nodules were evenly distributed along the ventricles in BL-PVNH, but tended to cluster around the trigone in UL-PVNH. Compared to controls, both UL-PVNH and BL-PVNH patients had increased cortical thickness and curvature in several regions of the brain. Increases in cortical thickness and curvature were found in the same hemisphere as the nodules in UL-PVNH, while in BL-PVNH cortical thickness increases were found bilaterally in the prefrontal cortex, and curvature increases were found bilaterally in the temporal lobe. In both cohorts, morphometric anomalies did not colocalize spatially with the nodules, as assessed by a visual inspection.

Significance. The quantitative approach we used here provides precise measurements of cortical thickness and curvature in PVNH, as opposed to qualitative and subjective visual descriptions. The hemispheric colocalization finding makes it more likely that both the heterotopic nodules and the cortical thickening are the results of the same disrupted developmental mechanism. Conversely, the absence of a spatial relationship between heterotopic nodules and morphometric anomalies suggests differential cellular signaling and migration pathways.

Résumé

Introduction. La corticogenèse humaine est divisée de façon générale en trois phases : la prolifération, la migration et l'organisation corticale. Ainsi, une faute dans l'une de ces phases mène à une malformation du développement cortical (MDC). En rendant possible la visualisation des MDC *in vivo*, l'imagerie par résonance magnétique (IRM) a été un instrument indispensable à leur classification. L'une de ces MDC est l'hétérotopie de la substance grise (HSG), définie par des masses de substance grise ectopique – que l'on dénomme « nodules » – qui contiennent des neurones n'ayant pas migré à leur destination prévue. Ces nodules se présentent variablement en termes d'emplacement, de latéralisation, de grosseur et d'étendue dans le cerveau.

Trois variétés d'HSG sont reconnues : l'hétérotopie nodulaire périventriculaire (HNPV), l'hétérotopie sous-corticale et l'hétérotopie en bandes. Le sujet de mon projet de maîtrise est spécifiquement l'HNPV. Comme toutes les variétés d'HSG, l'HNPV est hautement épileptogène, et l'épilepsie est souvent résistante aux médicaments.

Objectif. Quantifier les changements de courbure et d'épaisseur corticales dans l'HSG dans l'ensemble du cerveau et évaluer le rapport spatial entre les nodules et les régions de tels changements.

Méthodes. Nous avons obtenu des images pondérées en T1 (1 x 1 x 1 mm³) pour 41 patients atteints de l'HSG et pour 41 témoins sur des scanners 1.5T et 3T. Les patients ont

été séparés en ceux atteints de HSG unilatérale (UL) vs. ceux atteints de HSG bilatérale (BL). Les images ont été recalées dans l'espace stéréotaxique pour éliminer les différences de volume et d'orientation du cerveau. Nous avons manuellement délinéé l'emplacement des nodules et algorithmiquement extrait l'épaisseur et la courbure néocorticales pour l'ensemble du cerveau. Nous avons utilisé la modélisation linéaire de l'ensemble du cerveau pour statistiquement comparer les groupes.

Résultats. Les nodules étaient distribués uniformément le long des ventricules dans l'HSG BL, mais avaient tendance à former des grappes autour du trigone dans l'HSG UL. Par comparaison avec le groupe témoin, les patients atteints d'HSG UL et d'HSG BL avaient l'épaisseur et la courbure du cortex augmentées dans plusieurs régions du cerveau. Les augmentations de l'épaisseur et de la courbure du cortex ont été trouvées dans le même hémisphère que les nodules dans l'HSG UL, tandis que dans l'HSG BL les augmentations d'épaisseur corticale ont été trouvées bilatéralement dans le cortex préfrontal et les augmentations de courbure bilatéralement dans le lobe temporal. Dans les deux cohortes, les anomalies morphométriques ne semblaient pas avoir de rapport spatial avec les nodules, selon une inspection visuelle.

Conclusion. L'approche quantitative que nous avons utilisée ici fournit des mesures précises de l'épaisseur et de la courbure du cortex dans l'HSG, contrairement à des descriptions visuelles qualitatives et subjectives. La découverte d'une colocalisation hémisphérique entre les anomalies morphométriques et les nodules rend plus probable la possibilité que les anomalies ainsi que les nodules soient le résultat du même mécanisme

développemental endommagé. Inversement, l'absence d'un rapport spatial entre les nodules hétérotopiques et les anomalies morphométriques suggère des chemins distincts de signalisation et de migration cellulaires.

Table of Contents

Acknowledgements	
Related Publications	3
Abstract	4
Résumé	6
Table of Contents	9
List of Figures	11
List of Tables	11
Abbreviations	12
Chapter 1: Introduction	13
Chapter 2: Background	14
2.1. Steps of cortical development	14
2.2. Abnormal cortical development	
2.2.1. Focal Cortical Dysplasia	
2.2.2. Polymicrogyria	
2.2.3. Lissencephaly	
2.2.4. Gray matter heterotopia	
2.3. Magnetic resonance imaging	
2.4. Studies of the neocortex in gray matter heterot	оріа24
Chapter 3: Methods	25
3.1. Subjects	25
3.2. MRI acquisition and processing	25
3.3. Nodule labeling	
3.4. Statistical parametric probability maps	
3.5. Cortical thickness and curvature measurement	

3.6.	Statistical analysis	28
Chapter	4: Results	29
4.1	Group differences in age and gender	29
4.2	Nodule statistical parametric probability maps	30
4.3	Cortical thickness and curvature	30
Chapter	5: Discussion	36
5.1	Neocortical evaluation	36
5.2	Localization of nodules	38
5.3.	Relationship between cortical changes and nodules	39
5.4.	Limitations and future directions	41
Referen	ces	43

List of Figures

Figure 4.1 Regions of cortical thickening and SPAM map in BL-PVNH	. 32
Figure 4.2 Regions of cortical thickening and SPAM map in UL-PVNH	. 33
Figure 4.3 Regions of increased curvature and SPAM map in BL-PVNH	.34
Figure 4.4 Regions of increased curvature and SPAM map in UL-PVNH	. 35

List of Tables

Table 4.1 Age,	gender and lateral	lity information	29
------------------	--------------------	------------------	----

Abbreviations

BL Bilateral

CSF Cerebro-spinal fluid

FCD Focal cortical dysplasia

FLNA Filamin A

GABA Gamma-Aminobutyric acid

GM Gray matter

GMH Gray matter heterotopia

MCD Malformation of cortical development

MRI Magnetic resonance imaging

PMG Polymicrogyria

PVNH Periventricular nodular heterotopia

RFT Random field theory

SPAM Statistical parametric probability map

UL Unilateral

WM White matter

Chapter 1: Introduction

Periventricular nodular heterotopia (PVNH) is a highly epileptogenic malformation of cortical development (MCD). It is characterized by masses of gray matter ("nodules") consisting of neurons that have failed to migrate to their intended destination. Surgical treatment of this MCD may be challenging, as nodules are located deep in the white matter (WM), and they may have a complex relationship with the overlying cortex in terms of the epileptogenic network (Sisodiya, 2000).

Magnetic resonance imaging (MRI) has allowed clinicians to diagnose PVNH *in vivo* and has improved its classification with respect to other MCDs. Yet, aside from a few descriptive studies, there has been no attempt to evaluate whole-brain structural integrity in this condition. Moreover, assessing the relationship between heterotopic nodules and changes in the neocortex is likely to improve our understanding of the pathogenesis of this malformative process. The MRI-based measurements we propose, i.e., cortical thickness and curvature are validated, have biological as well as clinical relevance demonstrated in neurodegenerative diseases such as Alzheimer's disease (Donovan et al., 2014).

Hypothesis and aims

Based on several studies pointing to increased cortical thickness in other cortical malformations, we hypothesized that cortical thickness is increased in PVNH.

Aim 1: To investigate the whole-brain integrity of the neocortex in patients with PVNH

Aim 2: To assess the spatial relationship between nodules and neocortical changes

Chapter 2: Background

2.1. Steps of cortical development

Corticogenesis is the term used to describe the complex process whereby the cerebral cortex is formed. In the human embryo, the nervous system starts out as a single layer of neuroepithelial cells that lines the soon to be ventricular system. During an initial proliferative stage, each neuroepithelial cell within this layer is able to divide symmetrically – into two identical neuroepithelial cells. Thus, the neuroepithelial layer is able to grow at a fast pace, giving rise to an adequate number of progenitor cells (Jiang & Nardelli, 2015).

While growth of the neuroepithelial layer continues, a *marginal* layer starts to form at the surface of the neuroepithelium. This new marginal layer initially contains only the processes of neuroepithelial cells. The marginal layer will serve as a transit zone for migrating cells that originate from the neuroepithelial layer. While initially dividing only symmetrically, some cells in the neuroepithelium – named *stem* cells – eventually undergo asymmetrical division: one such cell will give rise to an identical stem cell as well as a neuroblast – a precursor to mature neural cells – which will migrate away from the ventricle and toward the marginal layer (Jiang & Nardelli, 2015). In later stages of proliferation, both daughter cells are neuroblasts. The neuroblasts will not necessarily reach the marginal layer; instead, they will pursue their migration in-between the neuroepithelial and marginal layers, forming a new layer termed the *mantle layer*. As more neuroepithelial cells convert to stem cells and neuroblasts, the mantle layer thickens rapidly (Nieuwenhuys

et al., 2008).

When neurogenesis is nearly complete, a fourth layer, the *subventricular zone*, gradually forms between the neuroepithelium and the mantle layer (Jiang & Nardelli, 2015). According to Nieuwenhuys et al. (2008), this fourth layer "gives rise to special classes of neurons and to all types of macroglial elements, with the possible exception of ependymal cells." They point out that the subventricular zone is particularly well-developed in the telencephalic ganglionic eminences during neural development. This layer is important, as it becomes the largest source of neural stem cells in the adult brain (Capilla-Gonzalez et al., 2015).

As neurogenesis proceeds, young neuroblasts migrate through the mantle and marginal layers to reach their terminal position in the cortex. This migration is effected in one of two ways: through radial or through tangential migration. In radial migration, cells migrating from the neuroepithelium climb along a scaffold of structural cells denoted *radial glia* to reach the marginal layer. Radial glia extend from the neuroepithelium to the pial surface (Jiang & Nardelli, 2015). Radial migration paths are short, roughly corresponding to the distance from the ventricular surface to the pia. In tangential migration, cells migrate parallel to the pial surface, typically either through the marginal layer or through the superficial neuroepithelial layer. Tangential migration paths tend to be longer, and some neurons can migrate great distances to reach their destination. For neurons that migrate tangentially, radial migration precedes or follows the tangential migration phase in order for the neuron to reach the pial surface. Both migration modes occur throughout the brain and within the spinal cord (Nieuwenhuys et al., 2008).

During the sixth week of gestation, another layer, the *cortical plate*, starts to form between the marginal and pial layers. This new layer will mature to become the cortical gray matter. The gray matter of the human neocortex consists of six layers, simply numbered I through VI, layer VI being the deepest with respect to the pial surface (Raybaud & Widjaja, 2011). This cortical plate grows as more migrating cells reach it. The first cells to reach the cortical plate will organize to form layer VI, layer V will be formed next and so on up until layer II (layer I is the mature marginal layer and contains no cell bodies); thus, the layering of the cortical gray matter proceeds "inside-out" (Nieuwenhuys et al., 2008).

The bulk of neuroblast migration lasts until the 26th week of gestation. As migration completes and gray matter layers approach their terminal thickness, the mantle layer becomes the white matter of the mature cerebral cortex, while the neuroepithelial layer shrinks to become the neuroependyma, which in the end consists of a thin layer of cells lining the ventricles (Nieuwenhuys et al., 2008).

Neuroblasts which will settle in the neocortex originate both in the neuroepithelium of the neocortex itself as well as in the subventricular zone of the lateral and medial ganglionic eminences, which are temporary developmental structures. Neuroblasts produced in the neuroepithelium of the neocortex will mostly give rise to excitatory pyramidal neurons which use glutamate as a neurotransmitter, whereas neuroblasts produced in the ganglionic eminences will mostly divide into inhibitory local circuit neurons which use gamma-aminobutyric acid (GABA; Chu & Anderson, 2015; Nieuwenhuys et al., 2008). The neuroblasts which give rise to these latter inhibitory

neurons travel a long tangential trajectory to reach the neocortex (Paxinos & Mai, 2012). Nonetheless, Paxinos and Mai point out that at least some inhibitory interneurons result from proliferation in the neocortex.

Migration of all of the above cells is mostly effected and directed by the most abundant neurotransmitters in the brain: glutamate and GABA. Specifically, the interaction of glutamate and GABA with a variety of cell surface receptors controls radial migration, whereas tangential migration is due to the effect of metabotropic GABA-B receptors (Luhmann, Fukuda & Kilb, 2015).

2.2. Abnormal cortical development

As can be seen from the above description, corticogenesis is a complex process consisting of numerous steps. At every one of these steps, some mechanism may go wrong, potentially giving rise to a structural or functional abnormality of varying severity. Specifically structural abnormalities that are consequences of improper corticogenesis are referred to as malformations of cortical development (MCDs; Barkovich et al., 2012). MCDs are very diverse, and it is not uncommon to encounter more than one MCD within a single individual (Stutterd et al., 2014). To facilitate the work of scientists and clinicians in the field, attempts have been made to devise a classification of MCDs. The most widely accepted classification, devised by Barkovich et al. (2012), separates MCDs into three distinct but heterogeneous categories, based on the phase of corticogenesis: I. Malformations secondary to abnormal neuronal and glial proliferation or apoptosis; II.

Malformations due to abnormal neuronal migration; III. Malformations secondary to abnormal postmigrational development. Each of these categories contains a long array of MCDs.

Virtually all MCDs are well-documented causes of epilepsy, a condition that represents a significant cost to society, both in terms of finances and of public health. Given the wide range of recognized MCDs, discussing all of these is beyond the scope of the present thesis. However, some of the most epileptogenic MCDs merit a brief review.

2.2.1. Focal Cortical Dysplasia (FCD)

There are two distinct types of FCD. FCD type I is defined by abnormal cortical layering compromising the radial migration and maturation of neurons and/or the six-layered structure of the neocortex. It is classified as a malformation secondary to abnormal postmigrational development. FCD type II is defined as localized disrupted cortical lamination with specific cytologic abnormalities, namely dysmorphic neurons with or without balloon cells (Blümcke et al., 2011). It is classified as a malformation secondary to abnormal proliferation. While the imaging signature of FCD type I remains elusive, type II FCD presents on MRI as localized cortical thickening, blurring or signal intensity change within the cerebral cortex (Kabat & Król, 2012). For the latter, specifically, an abnormality located in the cerebral cortex might seem to contradict its classification as a disorder of proliferation, given that proliferation is a process that occurs within the neuroependymal layer. The explanation of this apparent discrepancy is simple: the cause of the disorder is strongly suggested to be neuronal and glial progenitor specifications, but because

migrational mechanisms are intact, the defective cells are able to reach the cerebral cortex, giving rise to the adult MRI phenotype (Barkovich et al., 2012). Epilepsy is a very frequent symptom of both types of FCD (Blümcke et al., 2011; Tassi et al., 2002; Tassi et al., 2010).

2.2.2. Polymicrogyria (PMG)

This malformation accounts for 20% of all MCDs (Leventer et al., 1999). It is characterized by an overfolding of the cerebral cortex – resulting in numerous small gyri – and by abnormal cortical structure and lamination (Stutterd & Leventer, 2014). PMG is classified as a malformation secondary to abnormal postmigrational development. It is generally accepted that PMG is not a single disorder, but rather a spectrum to which individual cases are assigned based on the severity of the observed overfolding and cortical dyslamination (Stutterd & Leventer, 2014). On MRI scans, it is most often located around the Sylvian fissure – in 61% of cases (Leventer et al., 2010) – and 91% of cases are bilateral (Stutterd & Leventer, 2014). A feature of PMG that helps distinguish it from other MCDs is stippling of the gray matter-white matter junction (Stutterd & Leventer, 2014). Like other MCDs, PMG is associated with epilepsy, in 78% of cases (Leventer et al., 2010).

2.2.3. Lissencephaly

The estimates of the prevalence of this MCD, a migrational disorder, range from 11.7 to 40 cases per million births (de Rijk-van Andel et al., 1991; Dobyns & Das, 2009). Like PMG, lissencephaly is not considered to be a distinct disorder, but rather a severity spectrum with differing neuroanatomical and clinical manifestations (Fry et al., 2014). Mild forms of

lissencephaly appear on MRI as abnormally wide and thick gyri or band heterotopia (band heterotopia is discussed below), whereas severe lissencephaly results in a complete lack of cortical folding and in a thick cortex. Other subtypes of lissencephaly include cobblestone, and X-linked (Barkovich et al., 2012). Lissencephaly is highly epileptogenic, as almost all patients eventually develop epilepsy. This condition is also often associated with severe developmental delay and intellectual disability, and the severity of the impairment correlates with the extent of agyria and cortical thickening (Barkovich et al., 1991; Cardoso et al., 2000).

2.2.4. Gray matter heterotopia (GMH)

The MCD that constitutes the focus of the present thesis is GMH. GMH is a heterogeneous group of cortical malformations that are classified as disorders of neuronal migration. It is characterized as masses of gray matter – referred to as "nodules" – consisting of neurons that have failed to migrate to their destination (Barkovich and Kuzniecky, 2000). The heterogeneity of GMH is reflected in the many ways of classifying it, with the classification often differing across studies: GMH has been shown to have genetic causes that affect progenitor proliferation in addition to migration, bringing into question its classification as a disorder of migration exclusively (Watrin et al., 2014). The types of GMH defined in Barkovich et al.'s classification are periventricular nodular heterotopia, subcortical heterotopia and band heterotopia. Each type is divided into subgroups, based on the phenotype and the severity of the malformation.

GMH cooccurs with epilepsy in 80-90% of patients (Guerrini and Dobyns, 2014).

Stereo electroencephalographic (SEEG) recordings – an invasive technique that measures electric potentials in deep regions of the brain – obtained before surgical intervention, as well as functional MRI-EEG studies have shown that at least some of the heterotopic gray matter nodules show spiking activity, suggesting a causal role in the generation of epileptic discharges (Watrin et al., 2014; Tyvaert et al., 2008; Kobayashi et al., 2006). Surgical resection of GMH nodules is rare: they tend to be deep in the white matter, and extensively spread (Sisodiya, 2004); however, at least some patients who do undergo complete surgical resection of nodules that show spiking stop having epileptic seizures. These case reports further support the notion that heterotopic gray matter plays a key – and likely causal – role in epileptogenesis.

2.2.4.1. Periventricular nodular heterotopia (PVNH)

In PVNH, the most frequent type of GMH, the ectopic masses of gray matter are immediately adjacent to the ventricles in contact with the neuroependyma (Watrin et al., 2014). Nodules can be of highly variable size, ranging from barely visible on MRI to those massive forms extending towards the cerebral cortex. There can be one or several nodules. The location ranges from being localized to a specific region of the ventricular periphery to being widely spread. They can be unilateral or bilaterally distributed (Sheen et al., 2004; Parrini et al., 2006). On MRI, the gray matter nodules appear as clusters of voxels of the same intensity as the cerebral cortex bordering the ventricles.

2.2.4.2. Subcortical heterotopia

The definition of subcortical heterotopia is very close to that of PVNH, with a few nuances: gray matter in subcortical heterotopia does not necessarily contact the ventricle – and therefore is not necessarily continuous with the neuroependyma –, and its pattern of spread is more curved (Barkovich et al., 2012). Apart from this difference, the number, size and extent of spread of subcortical heterotopia nodules are as variable as those of PVNH nodules.

2.2.4.3. Band heterotopia

This entity, also known as double cortex syndrome (Watrin et al., 2014), is different from both PVNH and subcortical heterotopia in that it is part of the spectrum of another disorder, namely lissencephaly (Barkovich et al., 2012). It is still, however, classified as a migrational disorder; specifically, it is a mild form of lissencephaly – classified as grade 5 or 6 lissencephaly (Dobyns & Truwit, 1995). It is characterized by long continuous stretches of gray matter within the white matter separated from the cerebral cortex by a thin layer of white matter; these gray matter bands run parallel to the ventricles without contacting these (Fry et al., 2014). The ectopic gray matter in band heterotopia often extends through all lobes, and is usually bilateral (Leventer et al., 2000). The overlying cortex is typically normal, but sometimes simplified (Fry et al., 2014). On MRI, like in the other two types of heterotopia, ectopic gray matter voxels are isointense with the cerebral cortex. The focus of our project is the most prevalent of the three subtypes of GMH, and the most common one diagnosed in adults, namely PVNH (Watrin et al., 2014).

2.3. Magnetic resonance imaging (MRI)

MRI is a standard medical and experimental imaging technique that reveals the macroscopic structure of the brain *in vivo*. High-resolution MRI has proven very useful in the diagnosis of MCDs, as most lesions are easily identified (Guerrini & Dobyns, 2014). As a consequence, MRI has been a driving force for the development of a classification for MCDs. MRI has likewise been useful in presurgical evaluation when MCDs cause uncontrollable epilepsy: the removal of lesions identified on MRI often leads to seizure-freedom or to a reduction in seizure burden (Lega et al., 2014).

In the present study, we will be using MRI to measure cortical thickness and curvature in PVNH, and comparing these to the same measures in healthy control subjects. Cortical thickness is a quantitative measure of the distance between corresponding points on the white matter and gray matter surfaces of the cerebral cortex (Lerch & Evans, 2005). Surface-based cortical thickness measurement lends a biologically meaningful metric as it reflects *in vivo* cortical morphology and preserves across-subject topology through vertex-wise correspondence. Scholtens et al. (2015) analyzed large human databases, comparing cortical thickness measurements obtained from T1-weighted MRI images against measurements of cortical thickness in histological slices, thus demonstrating the validity of cortical thickness measured on MRI. Curvature, on the other hand, refers to sulco-gyral patterns and is thought to be a footprint of cortical development (Voets et al., 2011). It is a quantitative measure obtained by dividing the perpendicular height of a vertex above the plane of best fit through its neighboring vertices by the average distance between all neighboring vertices and their centroid (Luders et al., 2005). MRI-based measures of

gyrification complexity thus provide unique tools to quantify altered folding related to MCDs.

2.4. Studies of the neocortex in GMH

Lee et al. (1997) performed one of the only histological studies of the overlying cortex in rat models of GMH, and found that the neocortex is thinned; they remark that the zone of cortical thinning surrounds the heterotopic tissue. Conversely, in a comprehensive review of MCDs in humans, Guerrini and Dobyns (2014) pointed out that thickening is observed in several MCDs; they report no thinning. Both descriptions were qualitative, with no measurements made. In the present study, given our results, we intend to lend support to the latter of these seemingly contradictory reports.

Hypothesis. Given that an animal model might not necessarily be representative of what happens in the human brain, and given the frequent findings of cortical thickening in other MCDs, we expect to observe cortical thickening in PVNH.

Purpose. The overall purpose of my Master's degree is to investigate whole-brain integrity of the neocortex in patients with PVNH using advanced imaging techniques targeting the neocortex. Specifically, we will measure cortical thickness and sulco-gyral curvature. Moreover, we will assess the spatial relationship between periventricular nodules and neocortical changes.

Chapter 3: Methods

3.1. Subjects

Our database consists of 41 patients with PVNH investigated at the Montreal Neurological Institute and 41 healthy controls. Diagnosis was determined by MRI assessment in all patients.

Patient and control cohorts were separated into two datasets based on the MRI hardware. The first dataset consists of 25 patients (12 males; 45±14 years; 19-77 years) and 25 age- and sex-matched healthy individuals (9 males; 36±10 years; 19-56 years) evaluated on a 1.5 Tesla scanner. The second dataset includes 16 patients (9 males; 30±9 years; 18-50 years) and 16 age- and sex-matched healthy individuals (10 males; 30±8 years; 20-48 years) evaluated on a 3 Tesla scanner.

We divided patients into UL-PVNH (1.5 Tesla: n=15; 3 Tesla: n=8) and BL-PVNH (1.5 Tesla: n=10; 3 Tesla: n=8) based on the laterality of nodules. These cohorts, together with the controls, were subsequently included in the morphometric analysis.

The Ethics Committee of the Montreal Neurological Institute and Hospital approved the study and written informed consent was obtained from all participants.

3.2. MRI acquisition and processing

T1-weighted MRI 1mm isotropic images at 1.5 Tesla were obtained on a Phillips Gyroscan

using a 3D Fast-Field-Echo sequence; T1-weighted 1mm isotropic images at 3 Tesla were acquired on a Siemens TimTrio using a 3D MPRAGE sequence.

Image preprocessing was uniform across both datasets and included automated correction for intensity non-uniformity and intensity standardization (Sled et al., 1998), as well as linear registration to a stereotaxic space based on the hemisphere-symmetric MNI-ICBM152 template (Fonov et al., 2009). The use of a symmetric template ensures an unbiased analysis when sorting hemispheres into ipsi- and contralateral with respect to the location of the nodule.

3.3. Nodule labeling

A single rater manually labeled heterotopic voxels of gray matter on the T1-weighted MRI. This was done for two reasons. Firstly, to generate a probability map for the location of the heterotopic nodules. Secondly, the automatic classifier may be misled by the presence of nodules in close proximity to the cerebral cortex, as nodules are isointense with the cortex, and therefore might be mistaken for cortex. Their presence may thus deform the surfaces extraction algorithm; we therefore instruct the algorithm to ignore voxels labeled as belonging to a nodule. To visualize individual brain scans and to label the nodules, we used the interactive software package DISPLAY developed at the Brain Imaging Center of the Montreal Neurological Institute, Canada.

3.4. Statistical parametric probability maps (SPAMs)

SPAMs provide an assessment of the likelihood of finding a nodule at a given locus in the brain. They are generated automatically by calculating – for every voxel – the percentage of patients in which the given voxel is labeled as a nodule. The resultant SPAM is three-dimensional, with a color attributed to each voxel as a function of the above percentage.

3.5. Cortical thickness and curvature measurements

We applied the Constrained Laplacian Anatomic Segmentation using Proximity algorithm to generate cortical surface models and to measure cortical thickness and curvature across 81,924 vertices (Kim et al., 2005). After the image is automatically classified into gray matter (GM), white matter (WM), and cerebro-spinal fluid (CSF), a surface mesh is iteratively warped to fit the WM-GM boundary. This boundary is expanded along a Laplacian map to fit the GM/CSF boundary. Surface-based registration improves anatomic vertex-correspondence across subjects. Importantly, the surface template is chosen to be hemisphere-symmetric based on the MNI152 dataset (Lyttelton et al., 2007). Thickness data are blurred using a surface-based diffusion kernel of 20 mm full-width at half-maximum. Cortical thickness is then calculated as the Euclidean distance between corresponding vertices on the WM and GM surfaces.

To measure curvature, we generated a surface model running at mid-distance between the inner and outer surfaces. We subsequently applied a barycentric smoothing with three iterations to reduce high frequency noise in vertex positions. Absolute mean curvature was calculated at each vertex to quantify changes in frequency and depth of sulcal and gyral folds, expressing local gyrification complexity. This metric was blurred with a surface-based kernel of 20 mm full-width at half-maximum.

3.6. Statistical analysis

We contrasted the cortical thickness and sulco-gyral curvature of each patient cohort (UL-PVNH, BL-PVNH) with those in healthy controls using a linear model.

To test for differences in mean age between patient and control groups, we used a two-sample t-test. To test for differences in gender distribution, we used a χ^2 test. Any significant intergroup differences of age or gender were controlled for in the linear model. In addition, field strength (3T vs. 1.5T) was always controlled for in the linear model, as is customary in imaging studies. Findings were corrected using random field theory (RFT; Worsley et al., 1999). Significance was always assessed at the $\alpha = 0.05$ level.

Patients with UL-PVNH nodules were analyzed relative to the hemisphere harboring the nodule. To eliminate potential confounds related to asymmetry, we normalized features (thickness, curvature) at each vertex using a z-transformation with respect to the corresponding distribution in controls (i.e., each patient's right/left feature was expressed as a vertexwise z-score with respect to right/left values in controls).

For all statistical analyses, we used the SurfStat toolbox for MatLab (R2014b, The Mathworks, Natick, MA; Worsley et al., 2009).

Chapter 4: Results

4.1 Group differences in age and gender

Age, gender and nodule laterality information is presented in **Table 4.1**. UL-PVNH patients and normal controls did not differ significantly in age (independent samples t-test; t(62) = 0.61) or gender (χ^2 ; $\chi^2(1) = 1.25$). BL-PVNH patients and normal controls did not differ significantly in gender ($\chi^2(1) = 0.28$), but did differ significantly in age (t(57) = 2.60); this latter difference was duly controlled for in the respective group comparison.

Table 4.1 | Age, gender and laterality information

	Age (years) mean (sd)	Gender (male/female)	PVNH side (right/left)
All PVNH (N = 41)	38.8 (14.4)	21/20	
Bilateral (N = 18)	42.8 (16.3)	7/11	
Unilateral (N = 23)	35.6 (12.2)	14/9	15/8
Controls (N = 41)	34.0 (9.7)	19/22	

PVNH = Periventricular nodular heterotopia, sd = standard deviation, N = number of subjects

4.2 Nodule SPAMs

Nodule SPAMs computed separately for BL-PVNH and UL-PVNH patients are presented graphically in **Figure 4.1b** and **Figure 4.2b**, respectively.

In BL-PVNH patients (**Figure 4.1b**), nodules occupy the entire length of the lateral ventricles and are evenly distributed along these ventricles in both hemispheres, as evidenced by the regions colored in red. There is, however, a larger cluster of high-likelihood of nodule location adjacent to the anterior horn of the right lateral ventricle than to that of the left lateral ventricle in BL-PVNH patients.

In UL-PVNH patients (**Figure 4.2b**), nodules occur more frequently at the ventricular trigone.

4.3 Cortical thickness and curvature

Cortical thickness results are shown in **Figure 4.1a** for BL-PVNH and in **Figure 4.2a** for UL-PVNH. Compared to controls, both BL-PVNH and UL-PVNH patients showed increased cortical thickness. In BL-PVNH, increases were located in the lateral and medial regions of the prefrontal cortex, while in UL-PVNH patients, regions of increased cortical thickness were found in lateral and basal temporal lobe in the hemisphere ipsilateral to the nodules.

Curvature results are presented in **Figure 4.3a** for BL-PVNH and **Figure 4.4a** for UL-PVNH. Compared to controls, both cohorts showed increased curvature. In BL-PVNH

patients, regions of increased curvature were bilaterally distributed over the temporal lobe, mostly in the mesial, parahippocampal and posterior cingulate cortices, with a right-sided predominance. In UL-PVNH patients, the only region of increased curvature was observed in the posterior parahippocampal cortex in the hemisphere ipsilateral to the nodules.

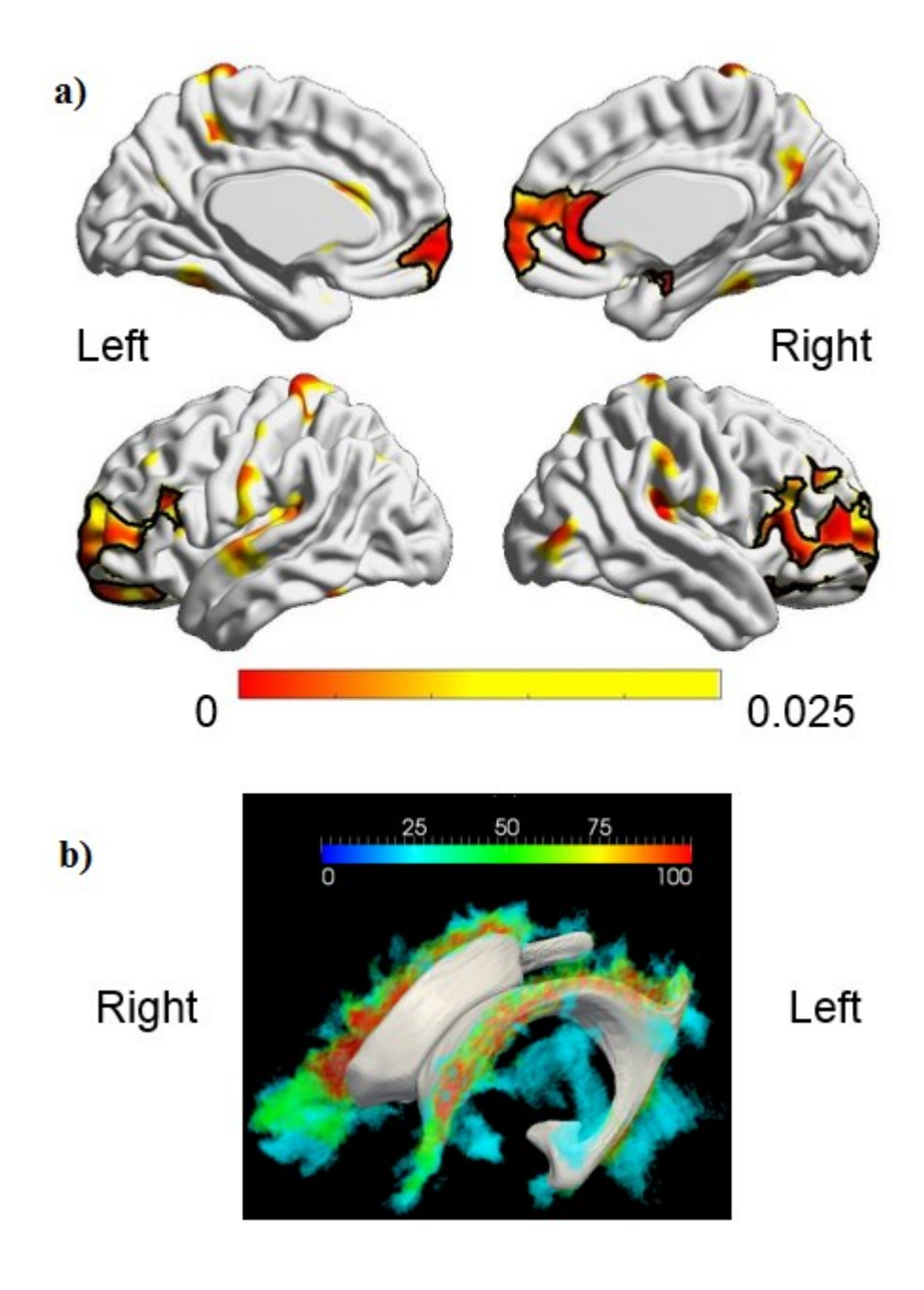


Figure 4.1 | Regions of cortical thickening and SPAM map in BL-PVNH

a) Regions of cortical thickening projected onto the MNI-ICBM152 brain template. The yellow-red gradient represents the p-value, red regions being the most significant. Regions with a black contour are RFT-corrected, and are the only ones that were considered significant for the purposes of the present study. b) SPAM map of BL-PVNH. Ventricles are white, the color gradient ranges from 0% to 100% and represents the percentage of patients in our sample that had a nodule at each periventricular locus.

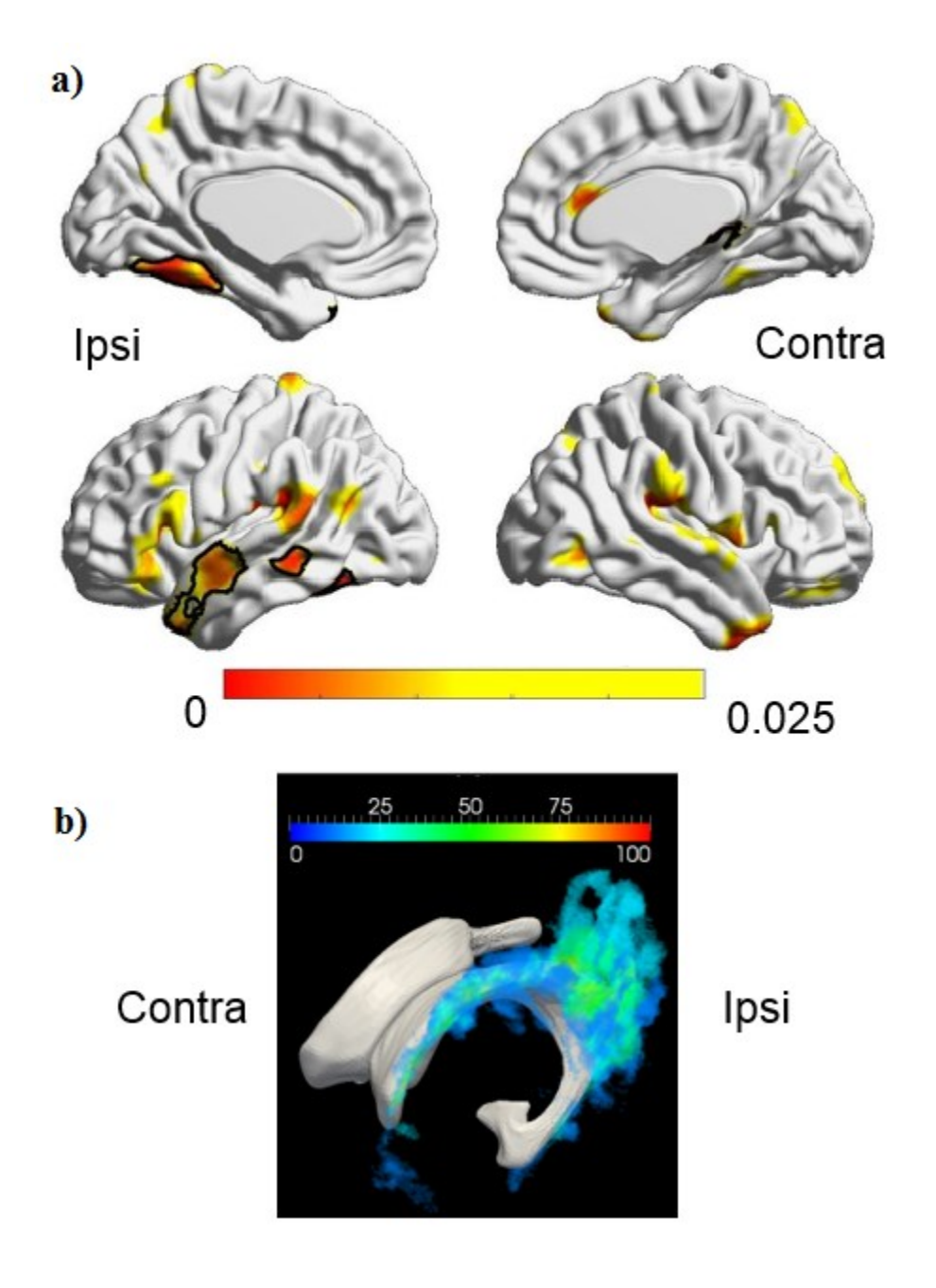


Figure 4.2 | Regions of cortical thickening and SPAM map in UL-PVNH

a) Regions of cortical thickening projected onto the MNI-ICBM152 brain template. The yellow-red gradient represents the p-value, red regions being the most significant. Regions with a black contour are RFT-corrected, and are the only ones that were considered significant for the purposes of the present study. b) SPAM map of UL-PVNH. Ventricles are white, the color gradient ranges from 0% to 100% and represents the percentage of patients in our sample that had a nodule at each periventricular locus.

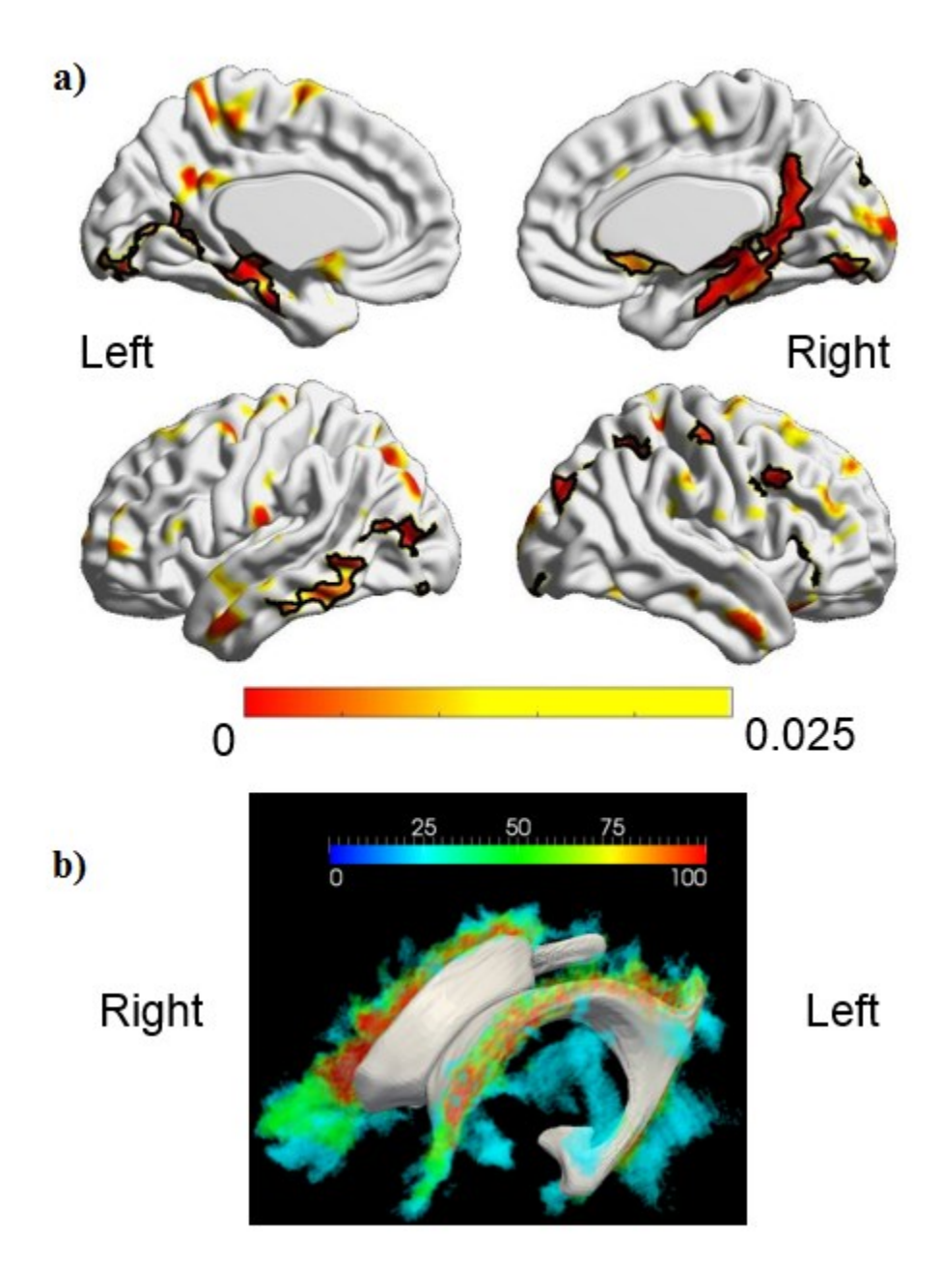


Figure 4.3 | Regions of increased curvature and SPAM map in BL-PVNH

a) Regions of increased curvature projected onto the MNI-ICBM152 brain template. The yellow-red gradient represents the p-value, red regions being the most significant. Regions with a black contour are RFT-corrected, and are the only ones that were considered significant for the purposes of the present study. b) SPAM map of BL-PVNH. Ventricles are white, the color gradient ranges from 0% to 100% and represents the percentage of patients in our sample that had a nodule at each periventricular locus.

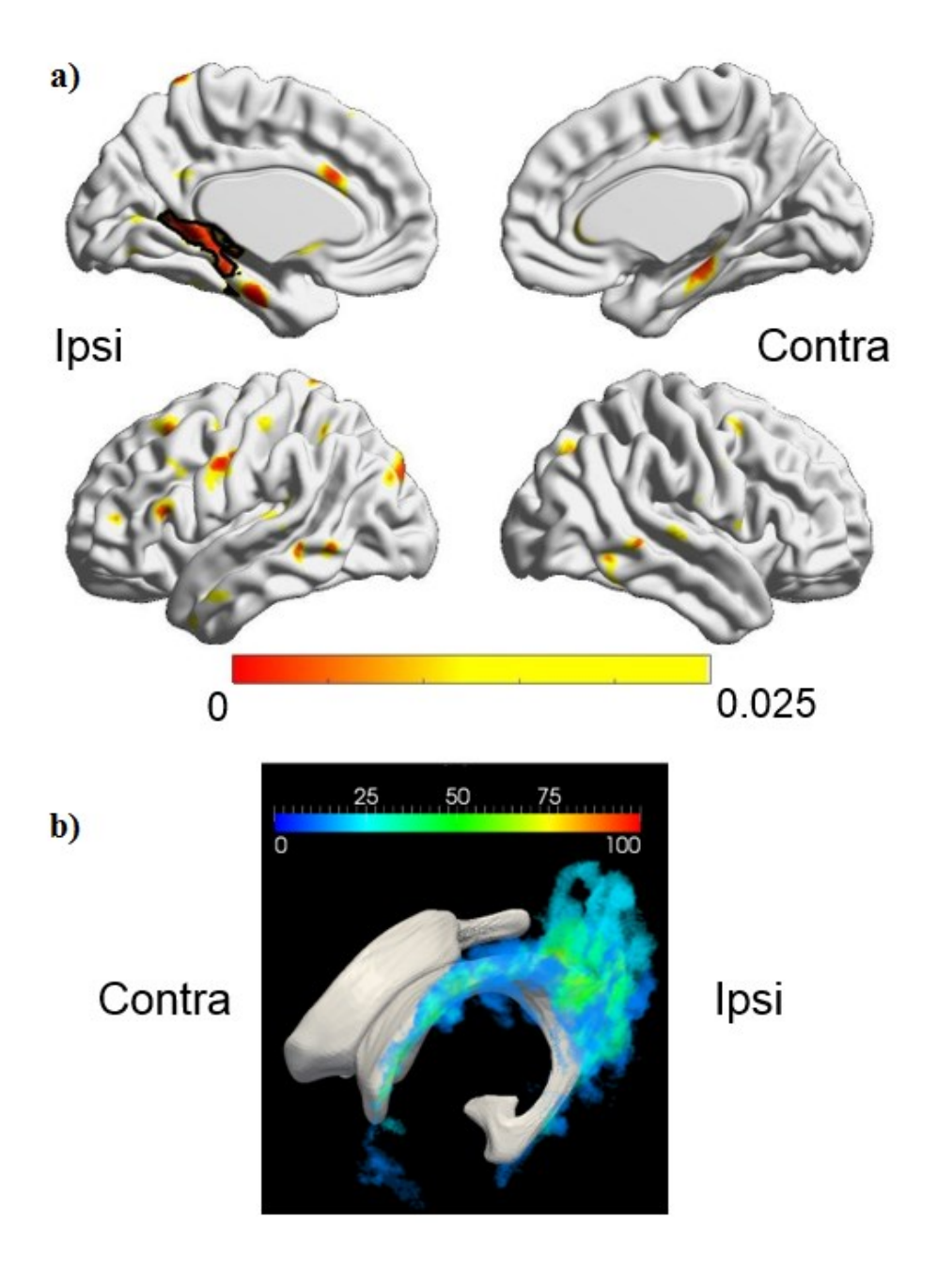


Figure 4.4 | Regions of increased curvature and SPAM map in UL-PVNH

a) Regions of increased curvature projected onto the MNI-ICBM152 brain template. The yellow-red gradient represents the p-value, red regions being the most significant. Regions with a black contour are RFT-corrected, and are the only ones that were considered significant for the purposes of the present study. b) SPAM map of UL-PVNH. Ventricles are white, the color gradient ranges from 0% to 100% and represents the percentage of patients in our sample that had a nodule at each periventricular locus.

Chapter 5: Discussion

5.1 Neocortical evaluation

This is the first analysis of whole-brain cortical thickness and cortical curvature in PVNH. Our results showed consistent increases in both measurements; no thinning or decreases in curvature were observed. Compared to controls, both UL-PVNH and BL-PVNH patients had increased cortical thickness and curvature in several regions of the brain. Increases in cortical thickness and curvature were found in the same hemisphere as the nodules in UL-PVNH, while in BL-PVNH cortical thickness increases were found bilaterally in the prefrontal cortex, and curvature increases were found bilaterally in the temporal lobe. In both BL and UL cohorts the increases did not seem to follow the pattern of nodule spread.

Increased cortical thickness in cases of GMH is a counterintuitive finding: given that GMHs are classified as diseases of migration, one would expect that the ectopic gray matter has failed to radially migrate to the overlying cortex. Such a hypothetical sequence of neurodevelopmental events would result in decreased cortical thickness. Yet, we observe an increase. Several mechanisms operating separately or jointly might explain an increased cortical thickness in PVNH. Firstly, cases of GMH might co-occur with arrested or reduced neural pruning before adulthood. It is well-documented that the human brain contains many more synapses at birth than it does in adulthood. This selective loss of synaptic connections that occurs from late gestation until late adolescence is referred to as neural pruning (Raznahan A et al., 2011). It is then easy to see how, if this pruning process is less thorough — or if it is arrested altogether at some point in brain development —, it may result in an

increased number of cells which can result in a thicker cortex. The causes for such an arrest of or reduction in pruning might be as variable as are the causes of PVNH itself: any variant of genetic or environmental alterations.

Another mechanism which might explain increased cortical thickness is a failure of migration of signaling cells such as Cajal-Retzius cells; these cells are among the first cells to appear in the developing brain. Their primary role is to emit the signaling molecule *reelin*. Reelin plays a key role in corticogenesis by attracting migrating neuroblasts and is known to be essential for cortical layering (Thom et al., 2011). It has a well-documented role in subcortical heterotopia: Thom et al. review several studies which have identified reelin-producing cells at the center of heterotopic gray matter. Among these is a study by Kubo et al. (2010) who have successfully reproduced a subcortical heterotopia-like phenotype in mice by injecting reelin during brain development, thus demonstrating a causal role in the formation of subcortical heterotopia. PVNH might likewise in some way be caused by reelin or any other type of signaling molecule that has failed to migrate to the marginal layer. If there is indeed a lack of such signaling molecules in the marginal layer of the overlying neocortex, cells migrating to the neocortex will be attracted to a lesser extent, resulting in a cortical mantle that is thicker or more curved, as we have observed.

Some cases of PVNH are known to be caused by environmental damage to the neuroependyma *in utero* (Barkovich et al., 2012). Such damage may, in addition to causing PVNH, disrupt molecular signaling mechanisms aimed at inhibiting progenitor cell proliferation. The result would be excessive proliferation, an increased number of migrating cells, and the increased cortical thickness or curvature we have observed. It is noteworthy

that a similar scenario could occur as a result of a mosaic (regional) genetic mutation; cases of Filamin A (FLNA) mosaicism in PVNH are documented in the literature (Guerrini et al., 2004). If the cause of PVNH is indeed a disruption of inhibitors of cell proliferation, the classification of PVNH as a disorder of migration is questionable; it would then be more appropriate to classify PVNH (and possibly other types of GMH) as disorders of cell proliferation.

Alternatively, the thickening we have observed may have been a consequence of glomeruloid blood vessels in the neocortex. In one case report of a female patient with BL PVNH, the authors examined the histology of the neocortex (Kakita et al., 2002). They noted a widespread distribution of glomeruloid vessels – vessels consisting of fused capillaries with an increased volume – which altered the cytoarchitecture of the neocortex, disturbing cortical layering and the columnar arrangement of neurons. This feature was most prominent in the frontal cortex, an observation mirrored by our finding of increased cortical thickness in the frontal lobes of patients with BL-PVNH.

5.2 Localization of nodules

In patients with UL-PVNH, the SPAM map in **Figure 4.2b** shows that the probability of the nodule appearing at any locus never exceeds ~75%, indicating less constancy in the location of nodules. However, it is evident from the SPAM map that nodules in UL-PVNH tend to be concentrated in the vicinity of the ventricular trigone, a zone defined by the posterior horn posteriorly, the body of the lateral ventricle anteriorly and the temporal horn

inferiorly. The ventricular trigone has been reported as a preferential location for nodules in a previous PVNH study (Donkol, Moghazy & Abolenin, 2012).

5.3. Relationship between cortical changes and nodules

One of our aims was to assess the spatial relationship between nodules and neocortical changes. In the specific case of patients with UL-PVNH, we observe increases in cortical thickness and curvature in the hemisphere ipsilateral to the nodule, and no change in the hemisphere contralateral to the location of the nodule. First and foremost, this hemispheric colocalization suggests that the cause of UL-PVNH is likely a combination of genetic and environmental factors; if the cause of UL-PVNH was exclusively genetic, we would be more likely to observe changes in cortical thickness in the contralateral hemisphere as well. On the other hand, if the cause of UL-PVNH is an environmental disturbance or a mosaic mutation, an abnormality such as cortical thickening is more likely to occur on the ipsilateral side, rather than on the contralateral side, as we have observed in our study. Though there are case reports of genetically caused PVNH in the literature (e.g. FLNA mutation), environmental causes have been documented and mosaic mutations are also possible (Barkovich et al., 2012). Moreover, the hemispheric colocalization finding makes it more likely that both the heterotopic nodules and the cortical thickening are the results of the same disrupted mechanism, as opposed to distinct mechanisms.

Another point worthy of emphasis is that the cortical thickening and increased curvature we have observed are not whole-brain phenomena (an example of a whole-brain

phenomenon is the band in subcortical band heterotopia), but are rather confined to discrete regions. Again, this finding argues against the fact that a genetic mutation is present in every cell; it is more likely that the damage that causes most cases of PVNH is either environmental or mosaic, affecting a specific region of the brain and causing a nodule to form and the cortex to thicken or curve focally.

Despite the lateralization of regions of increased cortical thickness and curvature with respect to the hemisphere harboring the nodule, increases do not occur exclusively in the cortex overlying the nodules in both UL-PVNH and BL-PVNH: in BL-PVNH, nodules are spread along the entire body of the lateral ventricles, whereas cortical thickening is evident only in the frontal lobes (**Figure 4.1**), while curvature is increased predominantly in the temporal lobes (**Figure 4.3**); in UL-PVNH, nodules are found predominantly adjacent to the ventricular trigone, whereas both cortical thickening and increased curvature are confined to the temporal lobe (**Figure 4.2** and **Figure 4.4**).

Assuming a single mechanism causes both nodules and increased cortical thickness and curvature, and assuming this mechanism is disrupted focally, the lack of overall colocalization of nodules with regions of increased cortical thickness or curvature would seem to suggest that the disrupted mechanism cannot be radial migration exclusively. However, radially migrating cells do not move strictly perpendicularly to the surface. Instead, they may deviate from a vertical path, moving sideways as they proceed towards the pial surface (Tabata & Nakajima, 2003). Therefore, an increase in cortical thickness or curvature that occurs in a region of the cortex that does not directly overlie the nodules may still be due to a disruption in radial migration. However, given that some regions of cortical

thickening and increased curvature occur in regions of the brain that are very far from regions where nodules are concentrated (the regions in the temporal lobe especially), a disruption of radial migration exclusively remains an unlikely explanation.

A disruption in tangential migration is a mechanism more likely to cause both nodules and cortical thickening along with increased curvature. The plausibility of tangential migration supports the Cajal-Retzius cells hypothesis, as these cells are known to migrate tangentially to spread evenly throughout the cortex (Borrell & Marín, 2006). Alternatively, other signaling cells that can migrate tangentially may be involved.

Given that the distribution of nodules as well as the patterns of thickening and increased curvature differ between UL-PVNH and BL-PVNH, we can conclude that the pathogeneses of UL-PVNH and BL-PVNH follow different patterns. This difference justifies the approach we chose in the present study: to analyze UL-PVNH and BL-PVNH separately.

5.4. Limitations and future directions

The present study, though it represents a substantial improvement over previous qualitative descriptions in the literature, has a number of limitations. Firstly, as previously stated, our analysis of whether morphometric changes we have observed in the cortex colocalize with nodules remains descriptive; the exception to this is our analysis of whether changes colocalize with nodules hemisphere-wise, which consists of a well-defined binary decision

(ipsi/contra). Future studies will ideally need to provide an operational definition of any colocalization variable – such as the overlying cortex – based on known models of migration.

Structural MRI morphometry cannot identify with certainty the mechanism responsible for the formation of nodules as well as for the cortical changes. There is need for detailed histochemical studies, which would provide insight into the actual mechanism whereby nodules are formed; into why and how thickening and increased curvature of the cortex occur; and into whether nodules and thickening or increased curvature have the same causative disturbed mechanism or are consequences of two distinct defective mechanisms.

References

- 1. Paxinos G, Mai JK. The Human Nervous System. London: Elsevier Academic Press, 2004.
- 2. Barkovich AJ, Koch TK, Carrol CL. The spectrum of lissencephaly: Report of ten patients analyzed by magnetic resonance imaging. Annals of Neurology 1991;30:139-146.
- 3. Barkovich AJ, Guerrini R, Kuzniecky RI, Jackson GD, Dobyns WB. A developmental and genetic classification for malformations of cortical development: update 2012. Brain 2012;135:1348-1369.
- 4. Blümcke I, Thom M, Aronica E, et al. The clinicopathologic spectrum of focal cortical dysplasias: A consensus classification proposed by an ad hoc Task Force of the ILAE Diagnostic Methods Comission. Epilepsia 2011;52(1):158-174.
- 5. Borrell V, Marín O. Meninges control tangential migration of hem-derived Cajal-Retzius cells via CXCL12/CXCR4 signaling. Nature Neuroscience 2006;10(9):1284-1293.
- 6. Cardoso C, Leventer RJ, Matsumoto N, et al. The location and type of mutation predict malformation severity in isolated lissencephaly caused by abnormalities within the LIS1 gene. Human Molecular Genetics 2000;9:3019-3028.
- 7. Capilla-Gonzalez V, Lavell E, Quiñones-Hinojosa A, Guerrero-Cazares H. Regulation of subventricular zone-derived cells migration in the adult brain. Advanced Experimental Medical Biology 2015;853:1-21.
- 8. Chu J, Anderson SA. Development of cortical interneurons. Neuropsychopharmacology 2015;40:16-23.

- 9. de Rijk-van Andel JF, Arts WF, Hofman A, Staal A. Niermeijer MF. Epidemilogy of lissencephaly type I. Neuroepidemiology 1991;10(4):200-204.
- 10. Dobyns WB, Das S. LIS1-addociated lissencephaly/subcortical band heterotopia. 2009. In: Pagon RA, Adam MP, Ardinger HH, Bird TD, Dolan CR, Fong CT, Smith RJH, Stephens K, editors. GeneReviews [Internet]. Seattle, WA: University of Washington, Seattle. Available from: http://www.ncbi.nlm.nig.gov/books/NBK5189/
- 11. Dobyns WB, Truwit CL. Lissencephaly and other malformations of cortical development: 1995 update. Neuropediatrics 1995;26:132-147.
- 12. Donovan NJ, Wadsworth LP, Lorius N et al. Regional cortical thinning predicts worsening apathy and hallucinations across the Alzheimer disease spectrum. Am J Geriatr Psychiatry 2014;22(11):1168-79.
- 13. Fonov V, Evans A, McKinstry R, Almli C, Collins D. Unbiased nonlinear average age-appropriate brain templates from birth to adulthood. Neuroimage 2009;47:S102.
- 14. Fry AE, Cushion TD, Pilz DT. The genetics of lissencephaly. American Journal of Medical Genetics 2014;166C:198-210.
- 15. Guerrini R, Marini C. Genetic malformations of cortical development. Experimental Brain Research 2006;173:322-333.
- 16. Jiang X, Nardelli J. Cellular and molecular introduction to brain development. Neurobiology of Disease 2015. doi:10.1016/j.nbd.2015.07.007. [Epub ahead of print]
- 17. Kabat J, Król P. Focal cortical dysplasia review. Polish Journal of Radiology 2012;77(2):35-43.
- 18. Kim JS, Singh V, Lee JK, et al. Automated 3-D extraction and evaluation of the inner and outer cortical surfaces using a Laplacian map and partial volume effect

- classification. Neuroimage 2005;59:3178-3186.
- 19. Kobayashi E, Bagshaw AP, Grova C, Gotman J, Dubeau F. Grey matter heterotopia: what EEG-fMRI can tell us about epileptogenicity of neuronal migration disorders. Brain 2006;129:366-374.
- 20. Kubo K, Honda T, Tomita K, et al. Ectopic Reelin induces neuronal aggregation with a normal birthdate-dependent "inside-out" alignment in the developing neocortex. Journal of Neuroscience 2010; 30:10953-10966.
- 21. Lee KS, Schottler F, Collins JL, et al. A genetic animal model of human neocortical heterotopia associated with seizures. Journal of Neuroscience 1997;17(16):6236-42.
- 22. Lega B, Mullin J, Wyllie E, Bingaman W. Hemispheric malformations of cortical development: surgical indications and approach. Child's Nervous System 2014;30:1831-1837.
- 23. Lerch JP, Evans AC. Cortical thickness analysis examined through power analysis and a population simulation. NeuroImage 2005:24:163-173.
- 24. Leventer RJ, Phelan EM, Coleman LT, Kean MJ, Jackson GD, Harvey AS. Clinical and imaging features of cortical malformations in childhood. Neurology 1999;53:1415-1427.
- 25. Leventer RJ, Pilz DT, Matsumoto N, Ledbetter DH, Dobyns WB. Lissencephaly and subcortical band heterotopia: molecular basis and diagnosis. Molecular Medicine Today 2000;6(7):277-84.
- 26. Leventer RJ, Jansen A, Pilz DT, et al. Clinical and imaging heterogeneity of polymicrogyria: A study of 328 patients. Brain 2010;133:1415-1427.
- 27. Luders E, Thompson PM, Narr KL, et al. A curvature-based approach to estimate

- local gyrification on the cortical surface. NeuroImage 2006;29:1224-1230.
- 28. Luhmann HJ, Fukuda A, Kilb W. Control of cortical neuronal migration by glutamate and GABA. Front Cell Neuroscience 2015;9:4.
- 29. Lyttelton O, Boucher M, Robbins S, Evans A. An unbiased iterative group registration template for cortical surface analysis. Neuroimage 2007;34:1535-44.
- 30. Nieuwenhuys R, Voogd J, van Huijzen C. The Human Central Nervous System. Berlin Heidelberg New York: Springer, 2008.
- 31. Parrini E, Ramazzotti A, Dobyns WB, et al. Periventricular heterotopia: phenotypic heterogeneityand correlation with Filamin A mutations. Brain 2006;129:1892-1906.
- 32. Raybaud C, Widjaja E. Development and dysgenesis of the cerebral cortex: malformations of cortical development. Neuroimaging clinics of North America 2011;21(3): 483-543.
- 33. Raznahan A, Lerch JP, Lee N, et al. Patterns of coordinated anatomical change in human cortical development: a longitudinal neuroimaging study of maturational coupling. Neuron 2011;72:873-884.
- 34. Scholtens LH, de Reus MA, van den Heuvel MP. Linking contemporary high resolution magnetic resonance imaging to the von Economo legacy: A study on the comparison of MRI cortical thickness and histological measurements of cortical structure. Human Brain Mapping 2015;36(8):3038-46.
- 35. Sheen VL, Basel-Vanagaite L, Goodman JR., et al. Etiological heterogeneity of familial periventricular heterotopia and hydrocephalus. Brain Development 2004;26:326-334.
- 36. Sisodiya SM. Surgery for malformations of cortical development causing epilepsy.

Brain 2000:123:1075-1091.

- 37. Sisodiya SM. Malformations of cortical development: burdens and insights from important causes of human epilepsy. Lancet Neurology 2004;3(1):29-38.
- 38. Sled JG, Zijdenbos AP, Evans AC. A nonparametric method for automatic correction of intensity nonuniformity in MRI data. IEEE Trans Med Imaging 1998;17:87-97.
- 39. Stutterd CA, Leventer RJ. Polymicrogyria: a common and heterogeneous malformation of cortical development. American Journal of Medical Genetics 2014;166C:227-239.
- 40. Tabata H, Nakajima K. Multipolar migration: the third mode of radial neuronal migration in the developing cerebral cortex. Jour. of Neuroscience 2003;31(23):9996-10001.
- 41. Tassi L, Colombo N, Garbelli R, et al. Focal cortical dysplasia: neuropathological subtypes, EEG, neuroimaging and surgical outcome. Brain 2002;125:1719-1732.
- 42. Tassi L, Garbelli R, Colombo N., et al. Type I cortical dysplasia: surgical outcome is related to histopathology. Epileptic Disorders 2010;12:181-191.
- 43. Tyvaert L, Hawco C, Kobayashi E, LeVan P, Dubeau F, Gotman J. Different structures involved during ictal and interictal epileptic activity in malformations of cortical development: an EEG-fMRI study. Brain 2008;131:2042-2060.
- 44. Voets NL, Bernhardt BC, Kim H, Yoon U, Bernasconi N. Increased temporolimbic cortical folding complexity in temporal lobe epilepsy. Neurology 2011;76:138-144.
- 45. Watrin F, Manent JB, Cardoso C, Represa A. Causes and consequences of gray matter heterotopia. CNS Neuroscience & Therapeutics 2014;21(2):112-122.
- 46. Worsley KJ, Andermann M, Koulis T, MacDonald D, Evans AC. Detecting changes

in nonisotropic images. Human Brain Mapping 1999;8:98-101.

47. Worsley K, Taylor J, Carbonell F, el al. SurfStat: A Matlab toolbox for the statistical analysis of univariate and multivariate surface and volumetric data using linear mixed effects models and random field theory. Neuroimage 2009;47:S102.